A Journal of the Gesellschaft Deutscher Chemiker

Angewandte International Edition GDCh Chemie

www.angewandte.org

Accepted Article

Title: Distannylated Monomer of Strong Electron-Accepting Organoboron Building Block: Enabling Acceptor-Acceptor Type Conjugated Polymers for n-Type Thermoelectric Applications

Authors: Changshuai Dong, Sihui Deng, Bin Meng, Jun Liu, and Lixiang Wang

To be cited as: *Angew. Chem. Int. Ed.* 10.1002/anie.202105127

Link to VoR: https://doi.org/10.1002/anie.202105127

WILEY-VCH

10.1002/anie.202105127

RESEARCH ARTICLE

WILEY-VCH

Distannylated Monomer of Strong Electron-Accepting Organoboron Building Block: Enabling Acceptor-Acceptor Type Conjugated Polymers for n-Type Thermoelectric Applications

Changshuai Dong,[a,b] Sihui Deng,[a,b] Bin Meng,*[a] Jun Liu,*[a,b] and Lixiang Wang[a,b]

[a] C. Dong, S. Deng, Dr. B. Meng, Prof. J. Liu, Prof. L. Wang
State Key Laboratory of Polymer Physics and Chemistry
Changchun Institute of Applied Chemistry, Chinese Academy of Sciences
Changchun 130022 (P. R. China)
E-mail: mengbin@ciac.ac.cn; liujun@ciac.ac.cn

[b] C. Dong, S. Deng, Prof. J. Liu, Prof. L. Wang
University of Science and Technology of China
Hefei 230026 (P. R. China)

Supporting information for this article is given via a link at the end of the document.

Abstract: Acceptor-acceptor (A-A) copolymerization is an effective strategy to develop high-performance n-type conjugated polymers. However, the development of A-A type conjugated polymers is challenging due to the synthetic difficulty. Herein, a distannylated monomer of strong electron-deficient double B←N bridged bipyridine (BNBP) unit is readily synthesized and used to develop A-A type conjugated polymers by Stille polycondensation. The resulting polymers show ultralow LUMO energy levels of -4.4 eV, which is among the lowest value reported for organoboron polymers. After n-doping, the resulting polymers exhibit electric conductivity of 7.8 S cm^{-1} and power factor of 24.8 μW m^{-1} K^{-2}. This performance is among the best for n-type polymer thermoelectric materials. These results demonstrate the great potential of A-A type organoboron polymers for high-performance n-type thermoelectrics.

Introduction

Conjugated polymers have received great attention because of their applications in organic opto-electronics, e.g. organic light emitting diodes (OLEDs), organic field-effect transistors (OFETs), organic solar cells (OSCs), organic photodetectors (OPDs), and organic thermoelectrics (OTEs).[1-3] They have the great advantages of flexibility and solution processing with low cost.[1] The majority of high-performance conjugated polymers are D-A type polymers consisting of electron-donating (D) building blocks and electron-accepting (A) building blocks.[4] Recently, great attention has been paid to A-A type conjugated polymers composed of all electron-accepting building blocks.[5-9] The development of n-type polymer semiconductors lags far behind that of p-type counterparts in terms of material diversity and device performance.[10,11] The A-A strategy is an effective route to design n-type polymer semiconductors.[6] Moreover, the absence of intramolecular charge transfer (ICT) characteristics in A-A type polymers would facilitate the more delocalized excitons/polarons, which favor the intrachain charge transport.[10a,12] Therefore, device performance of A-A type polymers have reached some milestone, i.e. 3 cm^2 V^{-1} s^{-1} electron mobility (μ_e) in OFETs,[5] 14% power conversion efficiency (PCE) in OSCs,[9] 50 μW m^{-1} K^{-2} power factor in n-type OTEs.[8a]

Despite of such promises, the development of A-A type polymers is challenging due to the synthetic difficulty.[6a] Although Suzuki polymerization, Ullmann reaction, Yamamoto polymerization, etc, have been used to synthesize A-A type polymers, the resulting polymers always show low molecular weights and high content of structural defects.[6a] High-performance A-A type polymers are always prepared by Stille polymerization employing di-stannyl monomer and di-bromo monomer.[6b,13] Di-stannyl monomers of electron-accepting building blocks are usually unstable and are difficult to synthesize.[14] Moreover, in Stille polycondensation, di-stannyl monomers of electron-accepting building blocks often show poorer reactivity than that of typical di-stannyl monomers of electron-donating building blocks, which are used in conventional D-A type polymers. As a result, A-A type conjugated polymers prepared by Stille polycondensation also often show low molecular weights.[6a,15] Therefore, it is important but challenging to design di-stannyl monomers of electron-accepting building blocks and prepare A-A type polymers with high molecular weight.

Scheme 1a shows the chemical structures of representative di-stannyl monomers of strong electron-accepting building blocks reported in literatures, e.g. naphthalene diimide[14a] and

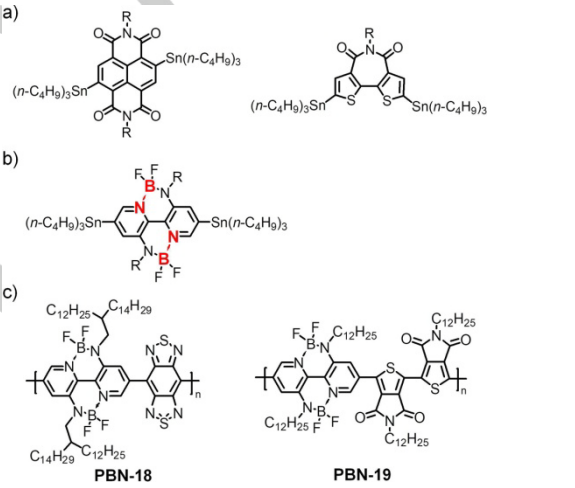

Scheme 1. Chemical structures of the di-stannyl monomers of electron-accepting building blocks reported a) in literatures and b) in this work, R = alkyl chains. c) Chemical structures of **PBN-18** and **PBN-19**.

bithiophene imide.[6b] These strong electron-accepting building blocks are based on imide unit. Boron-nitrogen coordination bond (B←N) is another strategy to design electron-accepting building blocks.[16] Our group has previously reported double B←N bridged bipyridine (BNBP) as another kind of strong electron-accepting building block.[17] In this manuscript, we report the di-stannyl monomer of BNBP unit (see Scheme 1b), which can be readily synthesized and show excellent reactivity in Stille polymerization, and enable the synthesis of A-A type conjugated polymers with high molecular weights. The previously reported D-A type polymers based on BNBP exhibit LUMO energy levels (E_{LUMO}) of -3.3 eV ~ -3.7 eV,[18] which are inadequate for n-doping and prevent n-type thermoelectric application.[10] In contrast, the A-A type polymers based on BNBP show E_{LUMO} of as low as -4.4 eV. After n-doping, the BNBP-based A-A type polymers exhibits electric conductivity (σ) of up to 7.8 S cm^{-1} and power factor (*PF*) of as high as 24.8 μW m^{-1} K^{-2}. This performance is among the highest for n-type polymer thermoelectric materials.[8,10,19] These results demonstrate the great potential of A-A type organoboron conjugated polymers for high-performance n-type thermoelectrics.

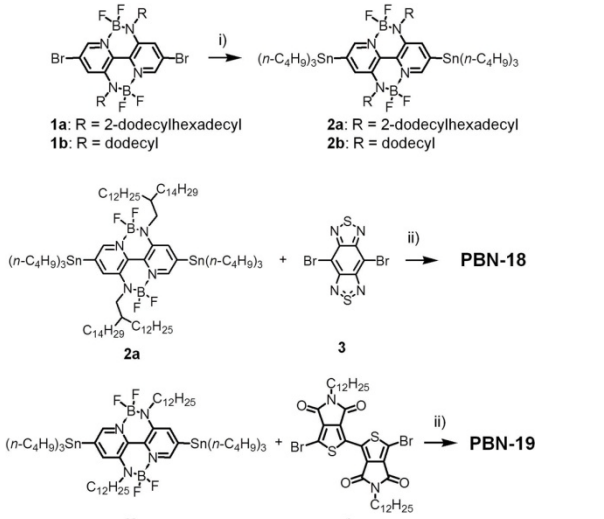

Scheme 2. Synthetic routes of **PBN-18** and **PBN-19**. (Reagents and conditions: i) $Sn_2(n\text{-}C_4H_9)_6$, $Pd_2(dba)_3$, P(*o*-tolyl)$_3$, toluene, 115 °C. ii) $Pd_2(dba)_3$, P(*o*-tolyl)$_3$, toluene, 115 °C)

Results and Discussion

BNBP Monomer Synthesis. The di-stannyl monomers of BNBP, **2a** and **2b**, were synthesized following the method reported by Marder et al.[14a] We have previously prepared the dibrominated BNBP (**1a** and **1b**). As shown in Scheme 2, the distannylated BNBP were prepared by Stille coupling of dibrominated BNBP and excessive hexabutylditin. The distannylated monomers of BNBP are very stable at ambient condition and can be purified by silica gel chromatography. Their chemical structures were confirmed by ^{1}H NMR and ^{13}C NMR.

Molecular Design of the Polymers. Scheme 1c shows the chemical structures of the two BNBP-based A-A type polymers, **PBN-18** and **PBN-19**. We select benzo[1,2-c:4,5-c']-bis[1,2,5]thiadiazole (BBT) and thieno[3,4-*c*]pyrrole-4,6-dione (TPD) dimer as the electron-accepting copolymerizing units to prepare the two A-A type organoboron polymers. BBT is well known for its ultrastrong electron-deficient property and quinoidal character.[20] Copolymerization of BNBP and BBT is expected to give ultralow LUMO energy level of the resulting A-A type polymer. TPD has been widely used to design p-type conjugated polymers for applications in high-performance OSCs and OFETs because of its medium electron-deficient property and planar configuration.[21] However, TPD has been rarely used to design n-type polymer semiconductors.[22] The copolymerization of BNBP unit with TPD dimer unit is expected to give a pseudo-straight configuration of the polymer backbone, which would facilitate ordered stacking of the polymer chains in solid state.[18a] To guarantee solubility of polymers, we attach branched 2-dodecylhexadecyl side chains to the BNBP unit in **PBN-18** and we use straight dodecyl side chains on both BNBP and TPD unit in **PBN-19** (Scheme 1c).

Synthesis and Characterization. The synthetic routes to the two polymers are illustrated in Scheme 2. The synthetic procedures are provided in the Supporting Information. The dibrominated monomer of BBT (**3**) was commercially available. The dibrominated monomer of dimeric TPD unit (**4**) was synthesized following the previously reported methods.[21] Stille polycondensation between **2a** and **3**, **2b** and **4** gave **PBN-18** and **PBN-19**, respectively. The chemical structures of the two polymers were confirmed by ^{1}H NMR and elemental analysis. Gel permeation chromatography (GPC) with 1,2,4-trichlorobenzene as the eluent at 150 °C indicates number-average molecular weights (M_n)/polydispersity indexes (PDI) of 25.0 kDa/2.53 for **PBN-18** and 15.1 kDa/2.95 for **PBN-19**, respectively (Table 1, Figure S1 of the Supporting Information). Most of A-A type conjugated polymers have M_n of lower than 10.0 kDa.[6a] The high M_n of **PBN-18** and **PBN-19** suggest excellent reactivity of the distannylated monomers of BNBP in Stille polycondensation. **PBN-18** and **PBN-19** are readily soluble in common organic solvents, e.g. chloroform, chlorobenzene. According to thermogravimetric analysis (TGA), the two polymers show excellent thermal stability with thermal decomposition temperatures (T_d) at 5% weight loss of higher than 330 °C (Table 1, Figure S2 of the Supporting Information).

DFT Calculations. To study the configuration of the polymer backbones of **PBN-18** and **PBN-19**, we performed density-functional theory (DFT) calculations at the B3LYP/6-31G** level with their dimers or tetramers.[23] Figure 1a and 1b show the optimized configuration of the dimers of **PBN-18** and **PBN-19**, respectively. The dihedral angle between the BNBP unit and the BBT unit (θ) in **PBN-18** is 33°, indicating twisted polymer backbone. For **PBN-19**, the dihedral angle between the BNBP unit and the TPD unit (θ_1) is 6°, the dihedral angle between the two adjacent TPD units (θ_2) is 0°, indicating coplanar conformation of the polymer backbone. Furthermore, the distance between the O atom of the TPD unit and the H atom of the BNBP unit ($d_{O\text{-}H}$ = 2.09 Å) is smaller than the sum of van der Walls radii of O and H (1.40 Å and 1.20 Å), indicating the presence of intramolecular hydrogen bonding. The distance between the O atom and the S atom of the two adjacent TPD units is 2.88 Å, which is obviously smaller than the sum of van

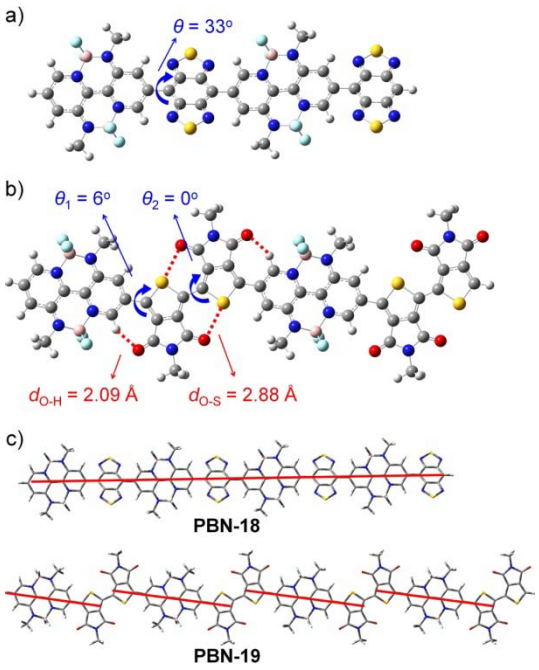

Figure 1. DFT-optimized geometry of the dimers of the polymer backbone of **PBN-18** a) and **PBN-19** b). The calculated dihedral angles between BNBP and BBT units (θ), between BNBP and TPD units (θ_1), between two adjacent TPD units (θ_2), and the distances of O-H ($d_{O\text{-}H}$) and O-S ($d_{O\text{-}S}$) are shown. c) Schematic illustration of the backbone shapes of the tetramers based on DFT calculation. All of the long alkyl chains have been replaced by methyl groups for simplification.

der Walls radii of O and S (1.40 Å and 1.84 Å). This suggests the presence of intramolecular non-covalent O-S interaction. The above results indicate that the coplanar conformation of **PBN-19** backbone is "locked" by the intramolecular O-H and O-S interactions.[24] This fully-locked coplanar conformation may lead to strong coupling between adjacent unit, improve the formation of extended excitons/polarons with long delocalized length, and finally improve intrachain charge transport.[10] As shown in Figure 1c, the tetramers of both the two polymer backbones show (pseudo-)straight configuration, which is expected to facilitate ordered stacking of polymer chains in solid state.[18a]

Opto-electronic Properties. The LUMO/HOMO energy levels (E_{LUMO}/E_{HOMO}) of **PBN-18** and **PBN-19** were estimated by cyclic voltammetry (CV) with their thin films. The cyclic voltammograms were shown in Figure 2a. The two polymers exhibit both reduction and oxidation waves. According to the onset potential of reduction/oxidation waves, the E_{LUMO}/E_{HOMO} of **PBN-18** and **PBN-19** are estimated to be -4.43/-5.88 eV and -4.02/-5.94 eV,

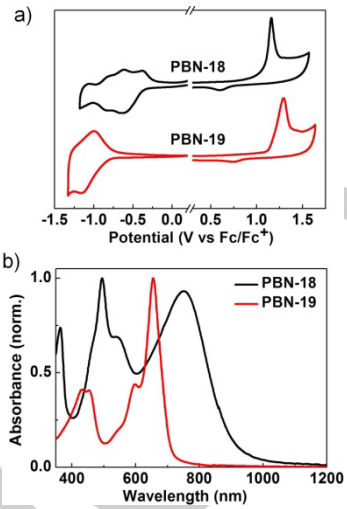

Figure 2. Cyclic voltammograms a) and UV-vis absorption spectra b) of **PBN-18** and **PBN-19** in thin films.

respectively (see Table 1). The E_{LUMO}/E_{HOMO} values of the two A-A type polymers are much lower than those of the BNBP-based D-A type conjugated polymers reported previously.[18] Moreover, the E_{LUMO} value of **PBN-18** is among the lowest reported so far for organoboron polymers.[25] The ultralow E_{LUMO} values are attributed to the strong electron-withdrawing capabilities of both the BNBP unit and the BBT/TPD copolymerization units. Such ultralow E_{LUMO} is considered to be very appealing for n-type thermoelectric applications. They may thermodynamically facilitate electron transfer between the polymers and n-dopants, and thus improve n-doping efficiency and enhance electric conductivity of the organoboron polymers.[10]

The ultraviolet-visible (UV-vis) absorption spectra of **PBN-18** and **PBN-19** in thin films are shown in Figure 2b, and the corresponding data are listed in Table 1. **PBN-18** shows two absorption bands with the maximum absorption wavelength (λ_{max}) at 495 nm and 753 nm, respectively. The onset absorption wavelength of **PBN-18** is 912 nm, corresponding to a narrow optical bandgap (E_g^{opt}) of 1.36 eV. The ultralow E_g^{opt} is attributed to the quinoidal character of BBT units in **PBN-18**.[20] **PBN-19** exhibits the maximum absorption wavelength of 655 nm. According to the onset absorption wavelength, the E_g^{opt} of **PBN-19** is estimated to be 1.76 eV.

To estimate the charge-transporting properties of the two polymers, we fabricated OFET devices with the top-gate/bottom-contact (TG/BC) structure of Si/SiO_2/Au/active layer/poly(methyl methacrylate) (PMMA)/Au (see Supporting Information). The active layers were spin-coated with the polymer solutions on Au deposited Si/SiO_2 substrates. Both the two organoboron

Table 1. Molecular weights (M_n), polydispersity indexes (PDI), thermal decomposition temperatures (T_d), energy levels, maximum absorption wavelength (λ_{max}), optical bandgap (E_g^{opt}), OFET electron mobilities (μ_e) of **PBN-18** and **PBN-19**.

Polymer	M_n [kDa]	PDI	T_d [°C]	E_{onset}^{red} [V][a]	E_{onset}^{ox} [V][a]	E_{LUMO} [eV]	E_{HOMO} [eV]	λ_{max} [nm]	E_g^{opt} [eV]	μ_e [$cm^2 V^{-1} s^{-1}$][b]
PBN-18	25.0	2.53	330	-0.37	1.08	-4.43	-5.88	495/753	1.36	3.3×10^{-6}
PBN-19	15.1	2.95	361	-0.78	1.14	-4.02	-5.94	655	1.76	2.9×10^{-2}

[a] Onset potential vs. Fc/Fc^+. [b] Average values from four devices.

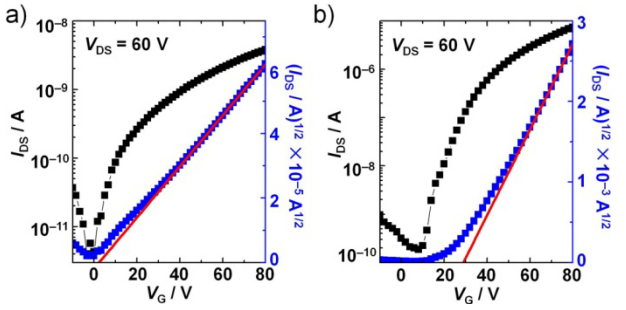

Figure 3. Transfer curves of the OFET device based on **PBN-18** a) and **PBN-19** b).

polymers exhibit unipolar electron transporting behaviors (Figure 3), which are ascribed to their extremely low E_{LUMO}/E_{HOMO} values. The electron mobilities (μ_e) of **PBN-18** and **PBN-19** are measured to be 3.3×10^{-6} cm^2 V^{-1} s^{-1} and 2.9×10^{-2} cm^2 V^{-1} s^{-1}, respectively. The unsatisfactorily low μ_e of **PBN-18** is probably ascribed to its twisted polymer backbone and poor stacking of polymer chains in thin film (vide infra).

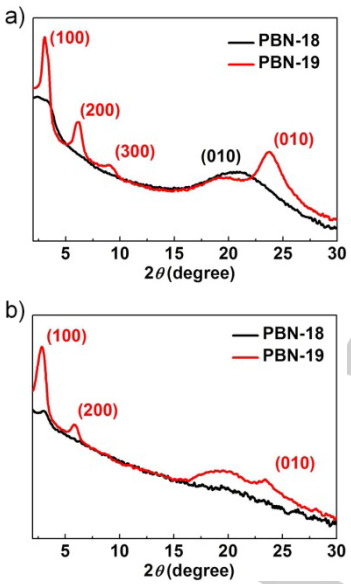

Figure 4. XRD patterns of the drop-cast films of **PBN-18** and **PBN-19** in the out-of-plane direction a) and the in-plane direction b).

Molecular Stacking in Thin Film. We performed X-ray diffraction (XRD) measurements with the drop-cast thin films of **PBN-18** and **PBN-19**. Figure 4 shows the XRD patterns of the two polymers in the out-of-plane direction and the in-pane direction. **PBN-18** shows broad (010) diffraction peak in the out-of-plane direction and weak (100) diffraction peak in the in-plane direction, suggesting poor packing of polymer chains with dominant face-on orientation. According to the (010) diffraction peak, the π-π stacking distance ($d_{π-π}$) is estimated to be 4.3 Å. The low crystallinity and relatively large $d_{π-π}$ of **PBN-18** are due to its twisted polymer backbone. For **PBN-19**, strong (100) and (010) diffraction peaks can be observed in both the out-of-plane direction and in-plane direction, suggesting mixed face-on/edge-

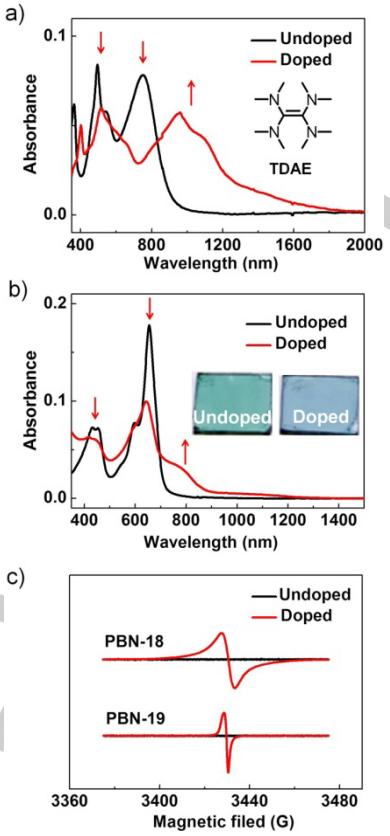

Figure 5. UV-vis-NIR absorption spectra of **PBN-18** a), **PBN-19** b) and EPR spectra of the two polymers c) in thin film before and after TDAE doping (t_{vapor} = 10 s for **PBN-18**, t_{vapor} = 3 h for **PBN-19**). The inset of a) is the chemical structure of TDAE. The inset of b) is the optical images of **PBN-19** films.

on orientation of the polymer chains. The bimodal orientation is appealing for thermoelectric applications because it favors accommodation of dopant or dopant cation in polymer film and facilitates charge transporting.[8a] According to the (010) diffraction peak, the $d_{π-π}$ of **PBN-19** is estimated to be 3.7 Å, indicating close packing of polymer chains. Besides, **PBN-19** shows high crystallinity because the (300) diffraction peak can be clearly observed in the out-of-plane direction. The mixed face-on/edge-on orientation, small π-π stacking distance and high crystallinity of **PBN-19** suggest excellent thermoelectric performance.[10]

n-Doping Behaviors. The ultralow E_{LUMO} of **PBN-18** and **PBN-19** motivate us to investigate their n-doping behaviors. To dope the two polymers, we used tetrakis(dimethylamino)ethylene (TDAE) (see the inset of Figure 5a, commercially available) as the n-dopant and exposed the polymer thin films to the TDAE vapor. The doping behaviors were studied by UV-vis-NIR absorption spectroscopy and electron paramagnetic resonance (EPR) spectroscopy (Figure 5). As shown in Figure 5a, the pristine **PBN-18** film shows two absorption bands at 495 nm and 753 nm. After exposure in TDAE vapor for ten seconds, the film shows greatly decreased absorbance at 495 nm and 753 nm accompanying with the appearance of a new strong absorption band at 900 nm - 1500 nm region. Similar trends are also observed for the absorption spectra of **PBN-19** upon TDAE

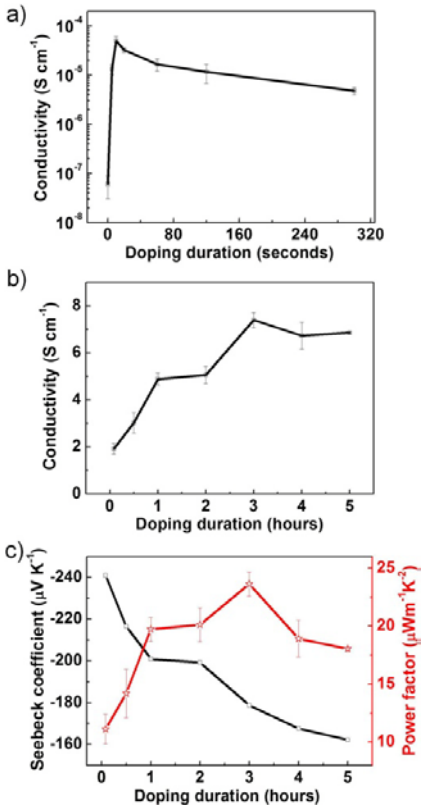

Figure 6. Electrical conductivities of a) **PBN-18** and b) **PBN-19** films exposed to TDAE vapor for different periods. c) Seebeck coefficients and power factors of **PBN-19** films exposed to TDAE vapor for different periods.

exposure for three hours (Figure 5b). The change of absorption spectra is clearly reflected by the color of the films (the inset of Figure 5b). The intensity of the new absorption band increases as the TDAE exposure time increases (Figure S4 of the Supporting Information). The new absorption bands at the low energy region of the two doped polymers are attributed to the (bi)polaron-induced transitions. The changes of absorption spectra imply effective n-doping of the two polymers upon TDAE exposure.[10] Compared with **PBN-19**, **PBN-18** shows more pronounced change in the absorption spectra even at shorter doping time, implying higher doping degree. This is possibly ascribed to the weaker crystallinity and less compact π-stacking of polymer chains of **PBN-18**, which facilitate permeation of TDAE molecules into the bulk film. The n-doping of the two polymers is confirmed by the EPR results. As shown in Figure 5c, the two pristine films both show no signals in the EPR spectra, while the films show strong signals after TDAE exposure, indicating the presence of unpaired electrons in the doped films. The n-doping behaviors are predominantly attributed to the ultralow E_{LUMO} of the two A-A type organoboron polymers.

Thermoelectric Performance. The electrical conductivity (σ) of the doped films of the two polymers was measured with the two-probe or four-probe method (Supporting Information, Figure S5). Figure 6a and 6b show the dependence of σ values on TDAE vapor exposure time of **PBN-18** and **PBN-19**, respectively. The optimal σ value of **PBN-18** is obtained at the exposure time of 10 seconds, while the optimal σ value of **PBN-19** is obtained with

Table 2. The optimal thermoelectric characteristics of **PBN-18** and **PBN-19** doped with TDAE.

Polymer	σ_{max} [S cm^{-1}]	$S^{[a]}$ [μV K^{-1}]	PF_{max} [μW m^{-1} K^{-2}]
PBN-18	6.6×10^{-5}	-	-
PBN-19	7.8	-178.8	24.8

[a] Seebeck values at PF_{max}.

the exposure time of 3 hours. The maximum σ values (σ_{max}) are evaluated to be 6.6×10^{-5} S cm^{-1} for **PBN-18** and 7.8 S cm^{-1} for **PBN-19**, respectively (Table 2). The relatively low σ value of doped **PBN-18** is ascribed to its low electron mobility. Noteworthy, the σ value of **PBN-19** is higher by nearly four times of magnitude than that in our first report of n-type organoboron thermoelectric polymer (σ = ca. 1×10^{-3} S cm^{-1}).[12a] **PBN-19** has moderate electron mobility, but shows high electrical conductivity after n-doping. The possible reason is that the charge carrier concentration of **PBN-19** after n-doping is very high.[10]

Then we estimated the Seebeck coefficients (S) of the doped **PBN-19** films by measuring the thermovoltage (V_{therm}) at a certain temperature difference (ΔT) (Supporting Information, Figure S6). We failed to collect the V_{therm} of the doped **PBN-18** film due to its low electrical conductivity. The doped **PBN-19** films exhibit negative Seebeck coefficients, suggesting electron-dominant transport. With increased n-doping time, the Seebeck coefficients of the doped **PBN-19** films gradually decrease (Figure 6c) because of the negative correlation between Seebeck coefficients and charge carrier concentration. The power factors (PF) of the doped **PBN-19** films were calculated with the formula of $PF = S^2\sigma$ (see Figure 6c). The maximum PF values (PF_{max}) is estimated to be 24.80 μW m^{-1} K^{-2} (Table 2). This value is higher by three times of magnitude than that of our first report of n-type organoboron thermoelectric polymer (PF = 0.02 μW m^{-1} K^{-2}).[12a] Most importantly, the PF value of **PBN-19** is fairly comparable to those of the mainstream solution-processed n-type polymer thermoelectric materials.[8,10,19] This result experimentally proves the promising application of A-A type organoboron polymers for efficient n-type organic thermoelectrics.

The morphology of the **PBN-19** films before and after n-

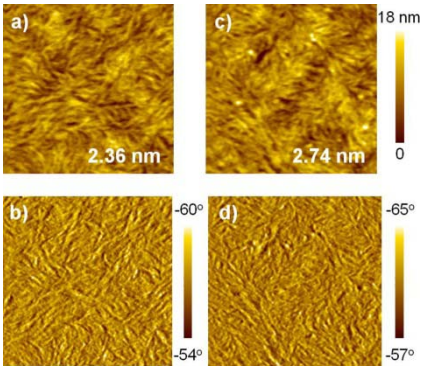

Figure 7. AFM height images (a,c) and phase images (b,d) of **PBN-19** thin films before doping (a,b) and after doping upon TDAE exposure for 3 hours (c,d). The root-mean-square (rms) surface roughness is provided in the height images. The scale size is 3 μm × 3 μm.

doping was studied using atomic force microscopy (AFM) and XRD. Figure 7 shows the AFM height and phase images of the films before and after n-doping. The pristine **PBN-19** film shows smooth surface with fibrous structures (Figure 7a,b). After exposed to TDAE vapor for 3 hours, the film surface become a little rougher while the fibrous nanostructure is preserved (Figure 7c,d). Concurrently, the XRD pattern of **PBN-19** keeps nearly unchanged after the n-doping (Figure S7 of the Supporting Information). Based on these results, we speculate that the doping with TDAE occurs predominantly at the amorphous region of the film and that the TDAE molecules do not interrupt the ordered stacking of polymer backbones. The doped morphology of **PBN-19** films supports its relatively high electrical conductivity and thermoelectric performance.

Conclusion

In conclusion, a distannylated monomer of strong electron-deficient BNBP is readily synthesized and used to develop A-A type conjugated polymers with high molecular weights. The A-A type organoboron polymers show ultralow E_{LUMO}s of -4.4 eV. After n-doping by TDAE, the A-A type organoboron polymers exhibit σ of up to 7.8 S cm^{-1} and *PF* of as high as 24.8 μW m^{-1} K^{-2}. This performance is among the highest for n-type polymer thermoelectric materials. These results demonstrate the great potential of A-A type organoboron conjugated polymers for high-performance n-type thermoelectrics.

Acknowledgements

The authors are grateful for the financial supports by the National Natural Science Foundation of China (No. 22075271, 21625403, 21875244, 21875241).

Keywords: doping • acceptor-acceptor type conjugated polymers • conducting materials • organic thermoelectrics • organoboron polymers

[1] a) A. J. Heeger, *Chem. Soc. Rev.* **2010**, *39*, 2354-2371; b) T. M. Swager, *Macromolecules* **2017**, *50*, 4867-4886; c) F. Huang, Z. Bo, Y. Geng, X. Wang, L. Wang, Y. Ma, J. Hou, W. Hu, J. Pei, H. Dong, S. Wang, Z. Li, Z. Shuai, Y. Li, Y. Cao, *Acta Polym. Sin.* **2019**, *50*, 988-1046.

[2] a) R. Kroon, D. A. Mengistie, D. Kiefer, J. Hynynen, J. D. Ryan, L. Yu, C. Müller, *Chem. Soc. Rev.* **2016**, *45*, 6147-6164; b) Q. Zhang, Y. Sun, W. Xu, D. Zhu, *Adv. Mater.* **2014**, *26*, 6829-6851; c) M. Goel, M. Thelakkat, *Macromolecules* **2020**, *53*, 3632–3642; d) H. Yao, Z. Fan, H. Cheng, X. Guan, C. Wang, K. Sun, J. Ouyang, *Macromol. Rapid Commun.* **2018**, *39*, 1700727.

[3] a) Z. R. Yi, S. Wang, Y. Q. Liu, *Adv. Mater.* **2015**, *27*, 3589-3606; b) K. Zhang, Z. C. Hu, C. Sun, Z. H. Wu, F. Huang, Y. Cao, *Chem. Mater.* **2017**, *29*, 141-148; c) Z. Zhang, M. Liao, H. Lou, Y. Hu, X. Sun, H. Peng, *Adv. Mater.* **2018**, *30*, 1704261.

[4] a) Y. Sun, H. Fu, Z. Wang, *Angew. Chem.* **2019**, *131*, 4488-4499; *Angew. Chem. Int. Ed.* **2019**, *58*, 4442-4453; b) H. Yao, L. Ye, H. Zhang, S. Li, S. Zhang, J. Hou, *Chem. Rev.* **2016**, *116*, 7397-7457; c) C. W. Zhao, Y. T. Guo, Y. F. Zhang, N. F. Yan, S. Y. You, W. W. Li, *J. Mater. Chem. A* **2019**, *7*, 10174-10199.

[5] Y. Wang, H. Guo, A. Harbuzaru, M. A. Uddin, I. Arrechea-Marcos, S. Ling, J. Yu, Y. Tang, H. Sun, J. T. López Navarrete, R. P. Ortiz, H. Y. Woo, X. Guo, *J. Am. Chem. Soc.* **2018**, *140*, 6095-6108.

[6] a) D. Qu, T. Qi, H. Huang, *J. Energy Chem.* **2021**, *59*, 364-387; b) Y. Shi, H. Guo, J. Huang, X. Zhang, Z. Wu, K. Yang, Y. Zhang, K. Feng, H. Y. Woo, R. Ortiz, M. Zhou, X. Guo, *Angew. Chem.* **2020**, *132*, 14557-14565; *Angew. Chem. Int. Ed.* **2020**, *59*, 14449-14457; c) Z. Yuan, B. Fu, S. Thomas, S. Zhang, G. DeLuca, R. Chang, L. Lopez, C. Fares, G. Zhang, J.-L. Bredas, E. Reichmanis, *Chem. Mater.* **2016**, *28*, 6045-6049.

[7] a) Y. Wang, T. Hasegawa, H. Matsumoto, T. Michinobu, *Angew. Chem.* **2019**, *131*, 12019-12028; *Angew. Chem. Int. Ed.* **2019**, *58*, 11893-11902; b) G. Kim, A. R. Han, H. R. Lee, J. Lee, J. H. Oh, C. Yang, *Chem. Commun.* **2014**, *50*, 2180-2183; c) K. Feng, H. Guo, J. Wang, Y. Shi, Z. Wu, M. Su, X. Zhang, J. H. Son, H. Y. Woo, X. Guo, *J. Am. Chem. Soc.* **2021**, *143*, 1539-1552.

[8] a) Y. Wang, K. Takimiya, *Adv. Mater.* **2020**, *32*, 2002060; b) S. Wang, H. Sun, T. Erdmann, G. Wang, D. Fazzi, U. Lappan, Y. Puttisong, Z. Chen, M. Berggren, X. Crispin, A. Kiriy, B. Voit, T. J. Marks, S. Fabiano, A. Facchetti, *Adv. Mater.* **2018**, *30*, 1801898; c) J. Liu, Y. Shi, J. Dong, M. I. Nugraha, X. Qiu, M. Su, R. C. Chiechi, D. Baran, G. Portale, X. Guo, L. J. A. Koster, *ACS Energy Lett.* **2019**, *4*, 1556-1564.

[9] H. Sun, H. Yu, Y. Shi, J. Yu, Z. Peng, X. Zhang, B. Liu, J. Wang, R. Singh, J. Lee, Y. Li, Z. Wei, Q. Liao, Z. Kan, L. Ye, H. Yan, F. Gao, X. Guo, *Adv. Mater.* **2020**, *32*, 2004183.

[10] a) B. Meng, J. Liu, L. Wang, *Nano Materials Science* **2020**, https://doi.org/10.1016/j.nanoms.2020.10.002; b) Y. Lu, J.-Y. Wang, J. Pei, *Chem. Mater.* **2019**, *31*, 6412-6423; c) Y. Sun, C.-A. Di, W. Xu, D. Zhu, *Adv. Electron. Mater.* **2019**, *5*, 1800825.

[11] a) B. Meng, Y. Ren, J. Liu, F. Jäkle, L. Wang, *Angew. Chem.* **2018**, *130*, 2205-2209; *Angew. Chem. Int. Ed.* **2018**, *57*, 2183-2187; b) H. Sun, X. Guo, A. Facchetti, *Chem* **2020**, *6*, 1310-1326; c) J. T. E. Quinn, J. Zhu, X. Li, J. Wang, Y. Li, *J. Mater. Chem. C* **2017**, *5*, 8654-8681; d) X. Long, J. Yao, F. Cheng, C. Dou, Y. Xia, *Mater. Chem. Front.* **2019**, *3*, 70-77.

[12] a) C. Dong, B. Meng, J. Liu, L. Wang, *ACS Appl. Mater. Interfaces* **2020**, *12*, 10428-10433; b) B. D. Naab, X. Gu, T. Kurosawa, J. W. F. To, A. Salleo, Z. Bao, *Adv. Electron. Mater.* **2016**, *2*, 1600004.

[13] a) R. Y. Zhao, C. D. Dou, Z. Y. Xie, J. Liu, L. X. Wang, *Angew. Chem.* **2016**, *128*, 5399-5403; *Angew. Chem. Int. Ed.* **2016**, *55*, 5313-5317; b) Y. Wang, M. Nakano, T. Michinobu, Y. Kiyota, T. Mori, K. Takimiya, *Macromolecules* **2017**, *50*, 857-864.

[14] a) L. E. Polander, A. S. Romanov, S. Barlow, D. K. Hwang, B. Kippelen, T. V. Timofeeva, S. R. Marder, *Org. Lett.* **2012**, *14*, 918-921; b) Z. Fei, Y. Han, J. Martin, F. H. Scholes, M. Al-Hashimi, S. Y. AlQaradawi, N. Stingelin, T. D. Anthopoulos, M. Heeney, *Macromolecules* **2016**, *49*, 6384-6393; c) L. Zhang, B. D. Rose, Y. Liu, M. M. Nahid, E. Gann, J. Ly, W. Zhao, S. J. Rosa, T. P. Russell, A. Facchetti, C. R. McNeill, J.-L. Brédas, A. L. Briseno, *Chem. Mater.* **2016**, *28*, 8580-8590.

[15] a) Y. Shi, H. Guo, M. Qin, Y. Wang, J. Zhao, H. Sun, H. Wang, Y. Wang, X. Zhou, A. Facchetti, X. Lu, M. Zhou, X. Guo, *Chem. Mater.* **2018**, *30*, 7988-8001; b) J. Chen, X. Zhuang, W. Huang, M. Su, L.-w. Feng, S. M. Swick, G. Wang, Y. Chen, J. Yu, X. Guo, T. J. Marks, A. Facchetti, *Chem. Mater.* **2020**, *32*, 5317-5326; c) Y. Shi, H. Guo, M. Qin, J. Zhao, Y. Wang, H. Wang, Y. Wang, A. Facchetti, X. Lu, X. Guo, *Adv. Mater.* **2018**, *30*, 1705745.

[16] a) C. Dou, J. Liu, L. Wang, *Sci. China Chem.* **2017**, *60*, 450-459; b) C. D. Dou, Z. C. Ding, Z. J. Zhang, Z. Y. Xie, J. Liu, L. X. Wang, *Angew. Chem.* **2015**, *127*, 3719-3723; *Angew. Chem. Int. Ed.* **2015**, *54*, 3648-3652; c) R. Zhao, J. Liu, L. Wang, *Acc. Chem. Res.* **2020**, *53*, 1557-1567.

[17] C. D. Dou, X. J. Long, Z. C. Ding, Z. Y. Xie, J. Liu, L. X. Wang, *Angew. Chem.* **2016**, *128*, 1458-1462; *Angew. Chem. Int. Ed.* **2016**, *55*, 1436-1440.

[18] a) X. Long, Z. Ding, C. Dou, J. Zhang, J. Liu, L. Wang, *Adv. Mater.* **2016**, *28*, 6504-6508; b) R. Zhao, Y. Min, C. Dou, B. Lin, W. Ma, J. Liu, L. Wang, *ACS Appl. Polym. Mater.* **2019**, *2*, 19-25; c) X. Long, C. Dou, J. Liu, L. Wang, *Macromolecules* **2017**, *50*, 8521-8528; d) R. Y. Zhao, C. D. Dou, J. Liu, L. X. Wang, *Chin. J. Polym. Sci.* **2017**, *35*, 198-206; e)

Z. Zhang, T. Wang, Z. Ding, J. Miao, J. Wang, C. Dou, B. Meng, J. Liu, L. Wang, *Macromolecules* **2019**, *52*, 8682-8689.

[19] a) J. Liu, G. Ye, H. G. O. Potgieser, M. Koopmans, S. Sami, M. I. Nugraha, D. R. Villalva, H. Sun, J. Dong, X. Yang, X. Qiu, C. Yao, G. Portale, S. Fabiano, T. D. Anthopoulos, D. Baran, R. W. A. Havenith, R. C. Chiechi, L. J. A. Koster, *Adv. Mater.* **2020**, *33*, 2006694; b) K. Shi, F. Zhang, C.-A. Di, T.-W. Yan, Y. Zou, X. Zhou, D. Zhu, J.-Y. Wang, J. Pei, *J. Am. Chem. Soc.* **2015**, *137*, 6979-6982; c) Y. Lu, Z.-D. Yu, Y. Liu, Y.-F. Ding, C.-Y. Yang, Z.-F. Yao, Z.-Y. Wang, H.-Y. You, X.-F. Cheng, B. Tang, J.-Y. Wang, J. Pei, *J. Am. Chem. Soc.* **2020**, *142*, 15340-15348; d) Y. Lu, Z.-D. Yu, H.-I. Un, Z.-F. Yao, H.-Y. You, W. Jin, L. Li, Z.-Y. Wang, B.-W. Dong, S. Barlow, E. Longhi, C.-a. Di, D. Zhu, J.-Y. Wang, C. Silva, S. R. Marder, J. Pei, *Adv. Mater.* **2021**, *33*, 2005946; e) X. Yan, M. Xiong, J.-T. Li, S. Zhang, Z. Ahmad, Y. Lu, Z.-Y. Wang, Z.-F. Yao, J.-Y. Wang, X. Gu, T. Lei, *J. Am. Chem. Soc.* **2019**, *141*, 20215-20221; f) H. Chen, M. Moser, S. Wang, C. Jellett, K. Thorley, G. T. Harrison, X. Jiao, M. Xiao, B. Purushothaman, M. Alsufyani, H. Bristow, S. De Wolf, N. Gasparini, A. Wadsworth, C. R. McNeill, H. Sirringhaus, S. Fabiano, I. McCulloch, *J. Am. Chem. Soc.* **2021**, *143*, 260-268.

[20] a) H. S. Oh, T.-D. Kim, Y.-H. Koh, K.-S. Lee, S. Cho, A. Cartwright, P. N. Prasad, *Chem. Commun.* **2011**, *47*, 8931-8933; b) G. Qian, B. Dai, M. Luo, D. Yu, J. Zhan, Z. Zhang, D. Ma, Z. Y. Wang, *Chem. Mater.* **2008**, *20*, 6208-6216.

[21] a) Y. Deng, Y. Chen, X. Zhang, H. Tian, C. Bao, D. Yan, Y. Geng, F. Wang, *Macromolecules* **2012**, *45*, 8621-8627; b) D. F. Yuan, S. M. Rivero, P. M. Burrezo, L. B. Ren, M. E. Sandoval-Salinas, S. J. Grabowski, D. Casanova, X. Z. Zhu, J. Casado, *Chem. Eur. J.* **2018**, *24*, 13523-13534; c) C. Zhao, F. Yang, D. Xia, Z. Zhang, Y. Zhang, N. Yan, S. You, W. Li, *Chem. Commun.* **2020**, *56*, 10394-10408.

[22] a) S. Liu, Z. Kan, S. Thomas, F. Cruciani, J.-L. Brédas, P. M. Beaujuge, *Angew. Chem.* **2016**, *128*, 13190-13194; *Angew. Chem. Int. Ed.* **2016**, *55*, 12996-13000; b) S. Liu, X. Song, S. Thomas, Z. Kan, F. Cruciani, F. Laquai, J.-L. Bredas, P. M. Beaujuge, *Adv. Energy Mater.* **2017**, *7*, 1602574; c) W. Wang, S. Yan, W. Lv, Y. Zhao, M. Sun, M. Zhou, Q. Ling, *J. Macromol. Sci. A* **2015**, *52*, 892-900.

[23] DFT calculations were performed using Gaussian 09: M. J. Frisch, et al. Gaussian 09, revision A.02; Gaussian, Inc.: Wallingford, CT, 2009. For details, see the Supporting Information.

[24] H. Huang, L. Yang, A. Facchetti, T. J. Marks, *Chem. Rev.* **2017**, *117*, 10291-10318.

[25] a) M. Grandl, J. Schepper, S. Maity, A. Peukert, E. von Hauff, F. Pammer, *Macromolecules* **2019**, *52*, 1013-1024; b) Y. Kawano, Y. Ito, S. Ito, K. Tanaka, Y. Chujo, *Macromolecules* **2021**, *54*, 1934-1942; c) J. Wakabayashi, M. Gon, K. Tanaka, Y. Chujo, *Macromolecules* **2020**, *53*, 4524-4532.

10.1002/anie.202105127

Entry for the Table of Contents

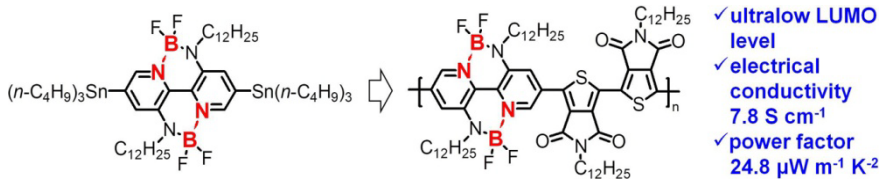

A distannylated monomer of strong electron-deficient double B←N bridged bipyridine (BNBP) is readily synthesized and used to develop acceptor-acceptor (A-A) type conjugated polymers by Stille polycondensation. The resulting polymers show ultralow LUMO energy levels and can be effectively n-doped, and thus lead to excellent thermoelectric performance.